

# LASER SURFACE PREPARATION OF EPOXY COMPOSITES FOR SECONDARY BONDING: OPTIMIZATION OF ABLATION DEPTH

Frank L. Palmieri<sup>\*</sup>, John Hopkins<sup>\*</sup>, Christopher J. Wohl<sup>\*</sup>, Yi Lin<sup>†</sup>, John W. Connell<sup>\*</sup>, Marcus A. (Tony) Belcher<sup>‡</sup>, and Kay Y. Blohowiak<sup>‡</sup>

<sup>\*</sup>NASA Langley Research Center, Hampton, VA 2368-2199

<sup>†</sup>National Institute of Aerospace, Hampton, VA 23666

<sup>‡</sup>The Boeing Company, Seattle, WA 98124-2207

## ABSTRACT

Surface preparation has been identified as one of the most critical aspects of attaining predictable and reliable adhesive bonds. Energetic processes such as laser ablation or plasma treatment are amenable to automation and are easily monitored and adjusted for controlled surface preparation. A laser ablation process was developed to accurately remove a targeted depth of resin, approximately 0.1 to 20  $\mu\text{m}$ , from a carbon fiber reinforced epoxy composite surface while simultaneously changing surface chemistry and creating micro-roughness. This work demonstrates the application of this process to prepare composite surfaces for bonding without exposing or damaging fibers on the surface. Composite panels were prepared in an autoclave and had a resin layer approximately 10  $\mu\text{m}$  thick above the fiber reinforcement. These composite panels were laser surface treated using several conditions, fabricated into bonded panels and hygrothermally aged. Bond performance of aged, experimental specimens was compared with grit blast surface treated specimens using a modified double cantilever beam test that enabled accelerated saturation of the specimen with water. Comparison of bonded specimens will be used to determine how ablation depth may affect average fracture energies and failure modes.

## 1. INTRODUCTION

Aircraft manufacturers rely on adhesive bonding for the assembly of primary structure to improve performance, reduce costs and meet rigorous safety regulations. Although airframe primary structures have been assembled with adhesive bonds for over 60 years, bonding technologies continue to develop rapidly as fiber reinforced plastic (FRP) becomes more prevalent.<sup>1,2</sup> Surface preparation has been recognized as a critical step to achieving a strong, durable, predictable adhesive bond. The surface preparation of composites is particularly challenging because of the broad range of surface conditions that are possible depending on the composite fabrication method and chemical composition.<sup>3</sup> Changes in bond performance can often be attributed to variation in surface preparation when using manual abrasion.<sup>1,4</sup> Also, detecting residual contaminants such as mold release agents or other materials used during composite fabrication can be challenging. Energetic techniques such as laser ablation and atmospheric pressure plasma to improve repeatability and quality of surface preparation are under evaluation by airframe manufacturers.<sup>5,6</sup> Preliminary studies by this group and others of laser ablation for surface preparation on both composites and metals have warranted a more detail understanding of how laser ablation affects bond performance.<sup>7-11</sup> A high fidelity laser ablation process is needed to control the depth of ablation and avoid exposing or damaging carbon fibers. Composite parts fabricated by various

methods and comprised of dissimilar fiber architectures are likely to have different resin contents on their surfaces. Thus a thorough understanding of the laser ablation parameters is needed to account for these differences, in order to sufficiently mature this technology for industrial use. The depth of penetration into a composite surface during laser ablation is a critical aspect of the surface preparation and is the subject of this report.

## **1.1 State-of-the-Art Surface Preparation**

For large-scale manufacturing, surface preparation of composites for secondary adhesive bonding is commonly accomplished by either mechanical abrasion (i.e., sanding, grit blasting) or the removal of a co-cured fabric known as peel ply.

### ***1.1.1 Mechanical abrasion***

Mechanical abrasion techniques such as sanding and grit blasting are labor intensive, difficult to automate, and are therefore sensitive to operator induced variability. Abrasion processes typically create debris that must be carefully removed from the faying surface and disposed of before bonding. When performed correctly, abrasive surface preparation results in strong bonds that have shown long term stability.<sup>12, 13</sup>

### ***1.1.2 Peel ply***

Peel ply is a layer of fabric that is applied as the final layer in a laminated, composite part before it is cured. The peel ply layer is removed from the cured composite part to expose a roughened, clean surface for bonding. Peel plies vary in terms of material composition and application method, and selection of a peel ply depends heavily on the composite content, molding process, adhesive type, and planned bonding process. Ideally, peel ply would eliminate the need for mechanical abrasion, but in some cases abrasion is required after peel ply removal.<sup>4, 13</sup>

## **1.2 Laser Surface Preparation**

Laser surface preparation is accomplished by ablation, which can be defined as vaporization of material due to intense laser irradiation. Organic polymer systems generally do not exhibit melting, re-freezing, and re-deposition processes that may be observed in other materials.<sup>6</sup> Ablation has been used to create high precision surface topography while simultaneously removing surface contaminants and modifying surface chemistry.<sup>6, 8-11</sup> The depth of ablation depends primarily on the laser fluence and number of passes or pulses directed at a point on the surface.<sup>8</sup> The ablation depth can be controlled by varying the average laser power, which is directly related to the laser fluence.<sup>14</sup> This report investigates the effect of laser power and therefore ablation depth on the adhesive bond performance of carbon fiber reinforced polymer (CFRP) composites.

## **1.3 Previously Reported Findings**

Previous work from these authors investigated laser ablation to prepare single lap shear specimens from CFRP substrates. The specimens were subjected to long-term aging at elevated temperature and humidity before being tested. Although laser power and ablation depth were not variables, it was found laser power must be monitored to assure repeatable specimen preparation. In this earlier study, samples prepared using laser ablation showed properties similar to those of control samples prepared using peel ply.<sup>14</sup>

## 1.4 Contents of this Report

The purpose of the current work is to investigate the role of laser power on surface preparation primarily in terms of ablation depth and subsequent effect on adhesive bond performance after hygrothermal aging. Modified double cantilever beam specimens were used to enable rapid saturation of the bondline. Ablation results, contact angle measurements, average fracture energies ( $G_{AVG}$ ), and failure mode data are presented.

## 2. EXPERIMENTATION

### 2.1 Material

Composite panels (CFRP, 30.5 cm x 30.5 cm) were prepared from two plies of unidirectional Torayca P2302-19 prepreg tape (T800H/3900-2 carbon fiber/toughened epoxy resin system) and cured in an autoclave at 177 °C (350 °F) and 690 KPa (100 psi). Release from the caul plate was accomplished using either high temperature polyimide film coated with Zyvax® Watershield or by using Airtech A4000 release film, respectively referred to as Zyvax and fluorinated ethylene propylene (FEP). Both release methods resulted in a nominally smooth panel surface that released easily from the mold. Eight-ply panels were fabricated using the same method, but Release Ease® 234 TFP (a fluoropolymer-coated cloth from Airtech) was used for mold release, which resulted in a textured surface. White aluminum oxide grit (180 mesh) was used for grit blasting of control specimens. Grit blasting was carried out in a non-recycling system with air at 138 kPa (20 psi). Adhesive used for bonding mechanical test specimens was Hysol EA9696 from Henkel Corporation with an areal weight of 0.39 kg/m<sup>2</sup> (0.08 PSF) on a polyester fiber carrier mat.

### 2.2 Laser Processing

Laser ablation was performed on a PhotoMachining, Inc. system with a Coherent®, Avia®, frequency tripled, Nd:YAG laser (2 W nominal pulsed output at 355 nm). CFRP panels were ablated with two patterns, according to Table 1, by direct irradiation with a focused beam. The nominal spot size was 25 μm, and the pulse frequency was 80 kHz. Lines, created by a series of overlapping pulses, were oriented along the fiber direction on each panel such that the ablation Pattern A was parallel to crack extension during testing. During ablation, the composite part was held stationary while the laser spot was scanned using a galvanometer. The write speed, 25.4 cm/s (10 in/s), and pulse frequency, 80 kHz, were held constant for all experiments. The average laser power was monitored after the final lens element using a thermopile sensor (model 3A-SH) and Nova II power meter from Ophir Spirocon LLC. The power was tuned to the power levels specified in Table 1 using a custom beam attenuator from PhotoMachining Inc.

Table 1: Experiment matrix for mechanical test specimen preparation.

Test Designation	Laser Pattern	Laser Power (mW)	Mold Release
1a	A	1000	Zyvax
2a	A	800	Zyvax
3a	A	600	Zyvax
4a	A	400	Zyvax
5a	A	200	Zyvax
1b	B	1000	Zyvax
2b	B	800	Zyvax
3b	B	600	Zyvax
4b	B	400	Zyvax
5b	B	200	Zyvax
4c	A	400	FEP
5c	A	200	FEP
Control	Grit Blast		Zyvax

Figure 1 shows a drawing of Patterns A and B written by the laser system. Pattern A is comprised of parallel lines with a center-to-center spacing (pitch) of 0.0254 mm (0.001 in). Pattern B is comprised of lines crossed at 90° to one another on 0.0508 mm (0.002 in) pitch to form a crosshatch pattern. Although the pitch of both patterns is fixed, the ablated trench width depends strongly on laser power, which influences areal coverage.

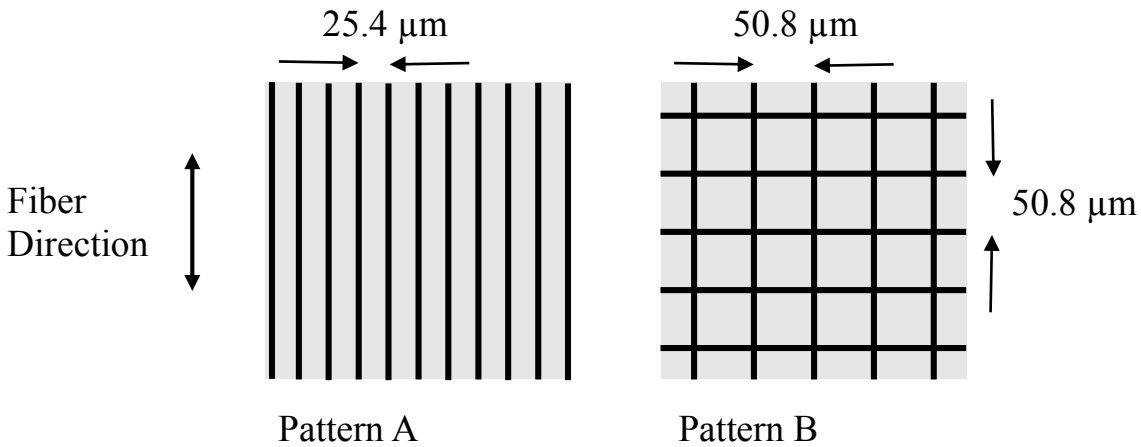


Figure 1: Laser ablation patterns showing beam path and line pitch for Patterns A and B.

### 2.3 Back-Bonded Double Cantilever Beam (BB-DCB) Specimen Preparation

A slight modification of ASTM D 5528 was used to prepare specimens for fracture toughness testing and enable rapid moisture saturation of the bonded joint.<sup>15,16</sup> The sample layout and specimen geometry is shown in Figures 2 and 3. The modification regarded the notched specimen

end for gripping and the bonding of 8-ply stiffeners after hygrothermal aging. Two-ply panels were laser-ablated and bonded with EA9696 in an autoclave at 121 °C (250 °F) and 0.34-0.68 MPa (50-100 psi). A 0.0125 μm film of FEP was used to create a precrack in the initial 76.2 mm of specimen length. The bonded panels were machined to 25.4 cm x 25.4 cm (10 in x 10 in) and then aged in an environmental chamber at 60 °C (140 °F) and 98% relative humidity for 14 days. Panels were weighed before and after aging to determine the mass of water absorbed. Aged panels and eight ply backer panels were prepared for back bonding by sanding with 80 grit aluminum oxide sand paper followed by wiping with isopropanol-wetted, lint-free cloths. Hysol EA9394 paste adhesive was applied to both sides of the bondline before curing in a heated press at 66 °C (150 °F) and 103 kPa (15psi). The stiffened panels were machined into 5, 25.4 mm x 241.3 mm (1 in x 9.5 in) specimens and notched (figure 3) to be mounted on a clevis-and-pin style grip. Back-bonding and machining was completed within 24 h of removal from the hygrothermal aging chamber.

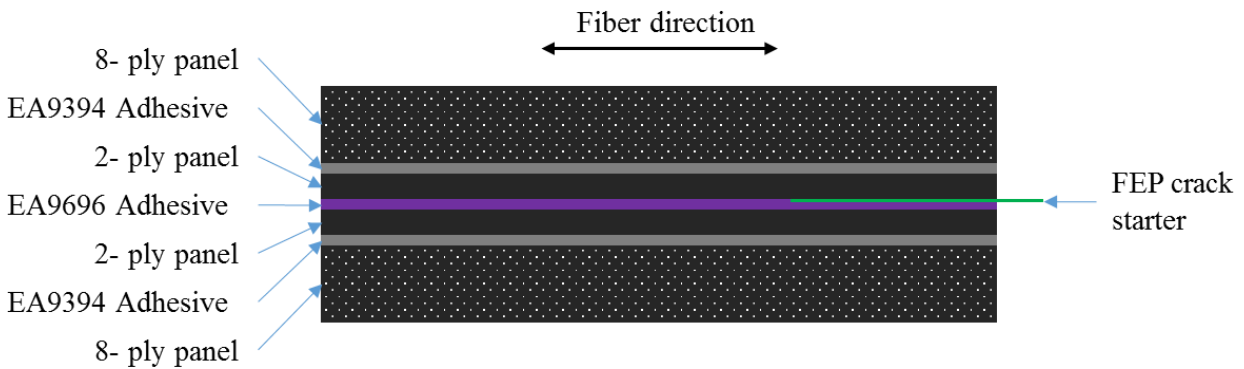


Figure 2: Layup of BB-DCB panels

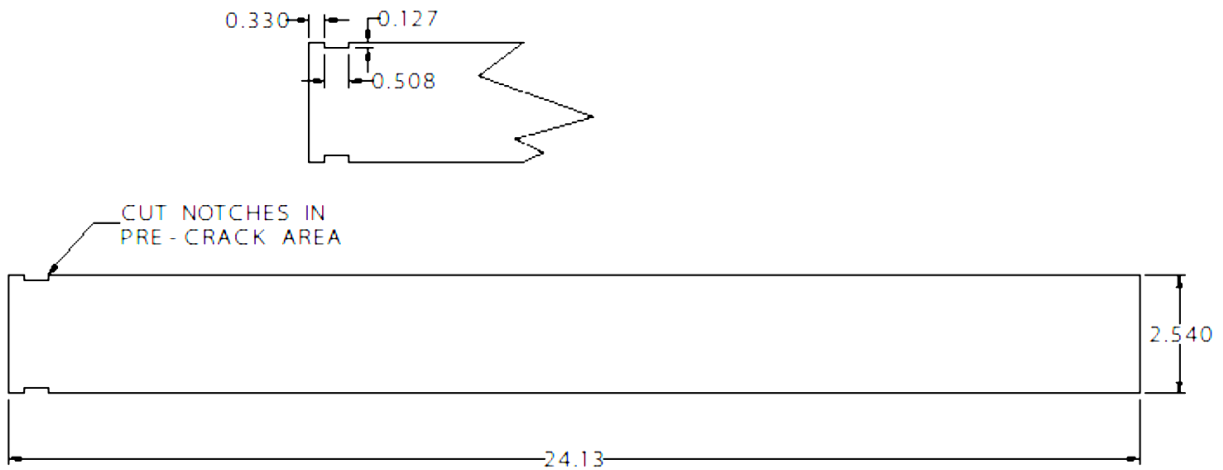


Figure 3: Drawing of BB-DCB specimen showing detail of notched end for installation in grip fixtures. Dimensions are in centimeters.

## 2.4 Mechanical Testing

Before testing, the bondline thickness was measured at four locations on both sides of each specimen using a Leica DM8000 M optical microscope to view the cross section. The cross section was then painted for contrast and the specimen installed in the grips. The specimen precrack was opened about 4 mm, which was needed for installation of the clevis grip fixtures. Using a clevis-and-pin fixture eliminated the need for additional fabrication and machining steps normally used to add tabs or blocks to the back of each specimen. The initial crack position was marked using a 10× magnifying glass. An Instron<sup>®</sup> 5848 Microtester equipped with a 500 N load cell was used to collect load and displacement data. The crosshead speed was 5 mm/min. For a complete test cycle, the free ends of the double cantilever beam were opened 20 mm to create a precrack, held briefly while the crack front was marked, returned to the initial gage length, and finally opened to 75 mm. If the beams were still joined at the end of the test, the final crack front was marked. The area method was used to calculate  $G_{AVG}$  for specimens that underwent controlled crack growth.

## 2.5 Contact Angle Measurement

Water contact angles were measured using a Surface Analyst<sup>™</sup> device from Brighton Technologies Group. For each two-ply panel, the contact angle was measured immediately after laser ablation and just prior to bonding. The time between ablation and bonding was consistently about 48 h. The measurements were made in at least three locations isolated from the area to be used for mechanical testing.

## 2.6 Electron Microscopy

Electron microscopy of the composite and neat resin plaques was performed with a JEOL JSM-5600 scanning electron microscope. Specimens were sputter coated with 30 to 40 Å of palladium/gold metal to reduce charging. Cross section images were collected to measure ablated trench width and depth.

# 3. RESULTS

## 3.1 Ablation Images

The diode laser used in this work produces a Gaussian beam that results in a bell-shaped trench when ablating a homogeneous material. Because of the Gaussian beam, high ablation power resulted in wider trenches as the depth increased. The cross section image in Figure 4 (left) shows a bell shaped trench produced at 600 mW in the surface resin of a CFRP panel. The top of a single carbon fiber is partially visible at the bottom of the trench. Figure 4 (right) shows an array of trenches produced using Pattern A at 200 mW. Unablated surface between the ablated trenches is clearly discernible.

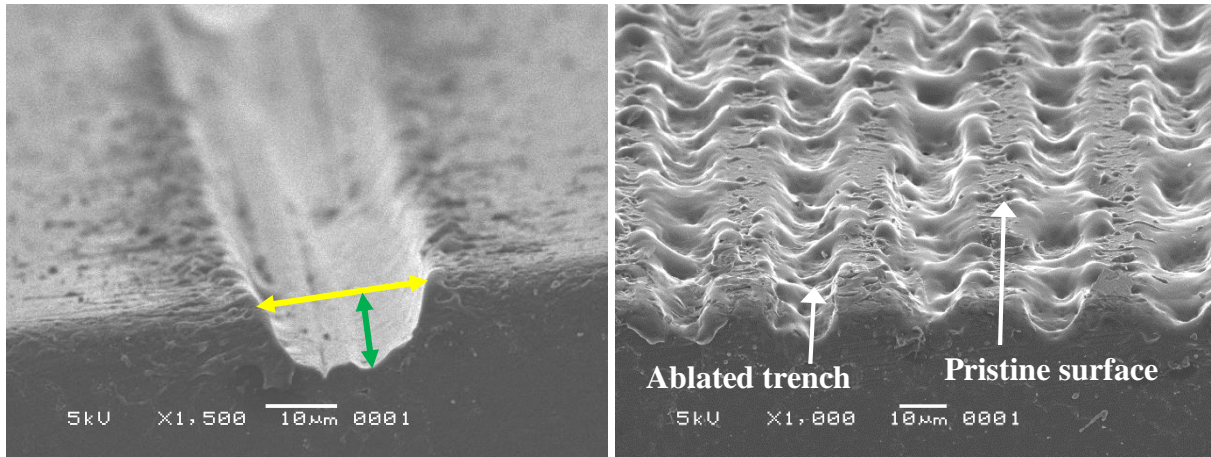


Figure 4: Cross-section SEM images of ablated, 2-ply composite panels prepared with Zyvax mold release. The isolated trench (left) was ablated at 600 mW. Arrows indicate method used to measure trench width (yellow) and depth (green). The array of trenches (right) was ablated with Pattern A at 200 mW.

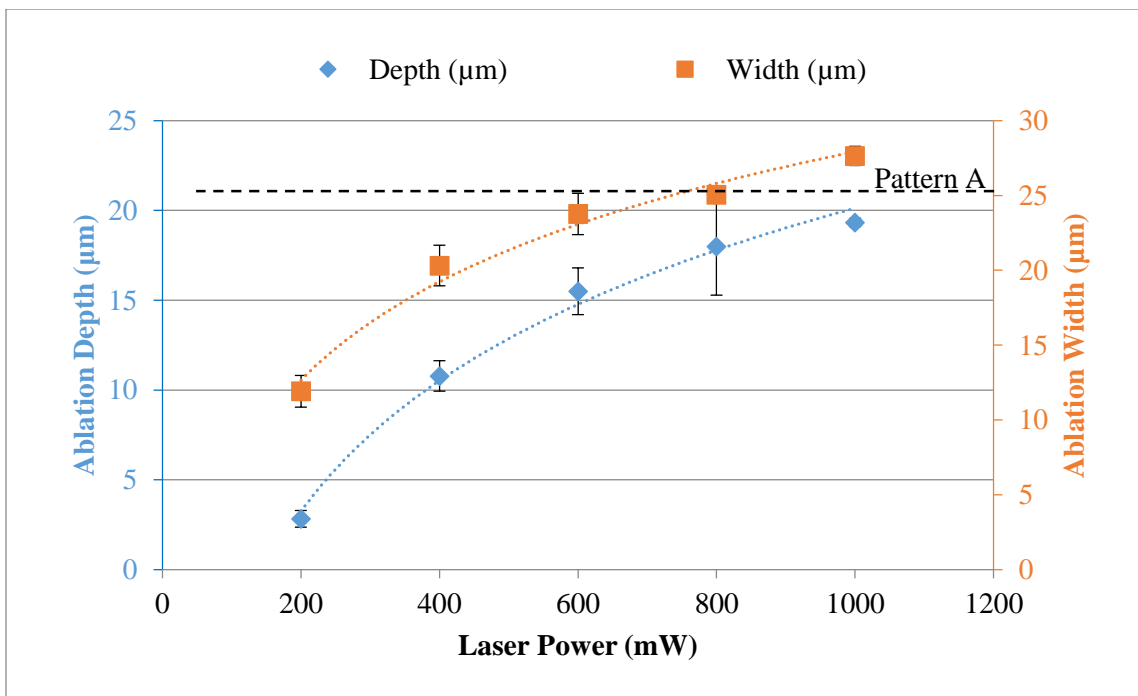


Figure 5: Ablation width and depth values measured from cross-section SEM images. The trend lines are logarithmic. The dashed line indicates the line pitch used in Pattern A.

The ablation depth and width were found to be highly repeatable for a single average laser power setting. As seen in Figure 5, the trench width was a logarithmic function of average laser power. The ablation threshold extrapolated from the width trend line was approximately 52 mW. Because the ablation patterns were produced with a constant pitch, the areal coverage is directly related to the ablation line width. Table 2 shows the calculated surface coverage based on measured line widths and pattern geometries. At high laser power, Pattern A resulted in complete areal coverage

because the trench width was greater than the pitch. As the laser power and line width decreased below 800 mW ( $23.8 \pm 1.2 \mu\text{m}$ ) the trenches became separated leaving some unablated surface area. Thus, to achieve full coverage at lower power setting requires a finer pitch. Pattern B produced less areal coverage at all ablation powers due to the dimensions of the crosshatch pattern.

Table 2: Calculated ablation areal coverage from ablation width and pattern pitch.

Power (mW)	Areal Coverage	
	Pattern A	Pattern B
200	47%	41%
400	80%	64%
600	94%	72%
800	99%	74%
1000	109%	79%

### 3.2 Water Contact Angle

Figures 6 and 7 show the water contact angle data collected from CFRP panels with Pattern A and Pattern B, respectively. The values measured immediately after ablation (0 h) decreased with increasing ablation power. Approximately 48 h elapsed between surface preparation and bonding. Contact angles were measured a second time on an unused area of each panel just prior to adhesive bonding. In general, these values slightly increased within 48 h after laser ablation for the CFRPs with both Patterns A and B. However, the contact angles of the CFRPs with Pattern A were generally similar to those of the control just prior to adhesive bonding whereas those of Pattern B were generally higher.

The elapsed time between laser ablation and adhesive bonding may have allowed residual contaminants in untreated areas to diffuse into treated areas, which increased the contact angle. The panels that were prepared using FEP film as mold release showed a lower contact angle at both ablation powers studied and did not change significantly during the hold time. This was attributed to the FEP film transferring less surface contamination than the Zyxax.



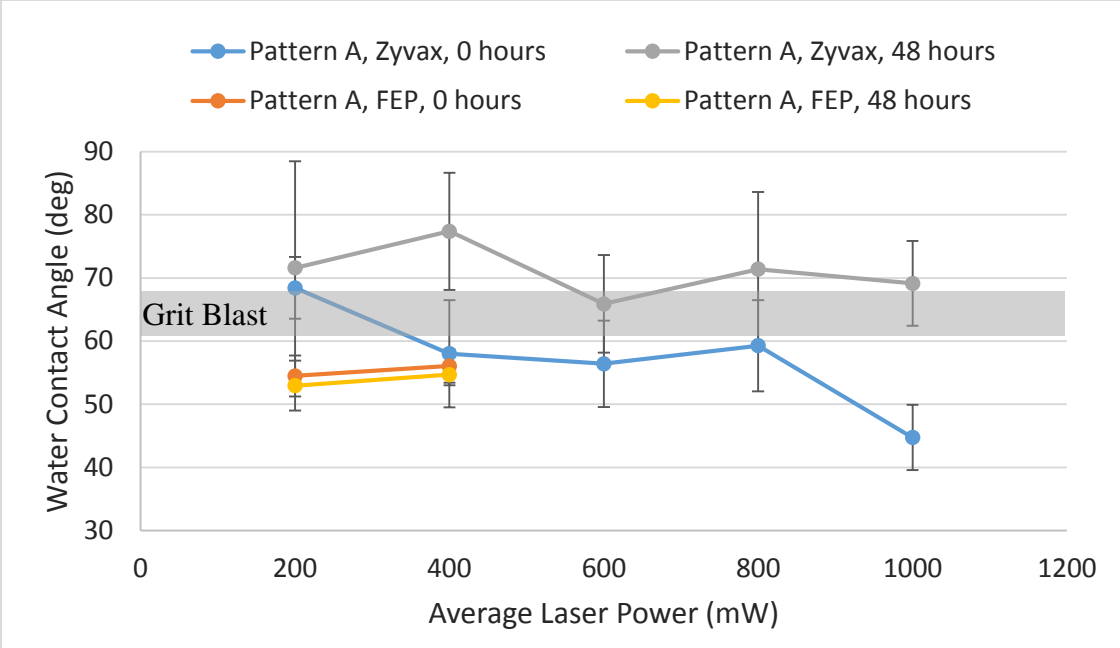


Figure 6: Water contact angle values on CFRP panels ablated with Pattern A immediately after ablation and just prior to adhesive bonding. The gray shaded area indicates the contact angle range measured for the control sample that was prepared by grit blast.

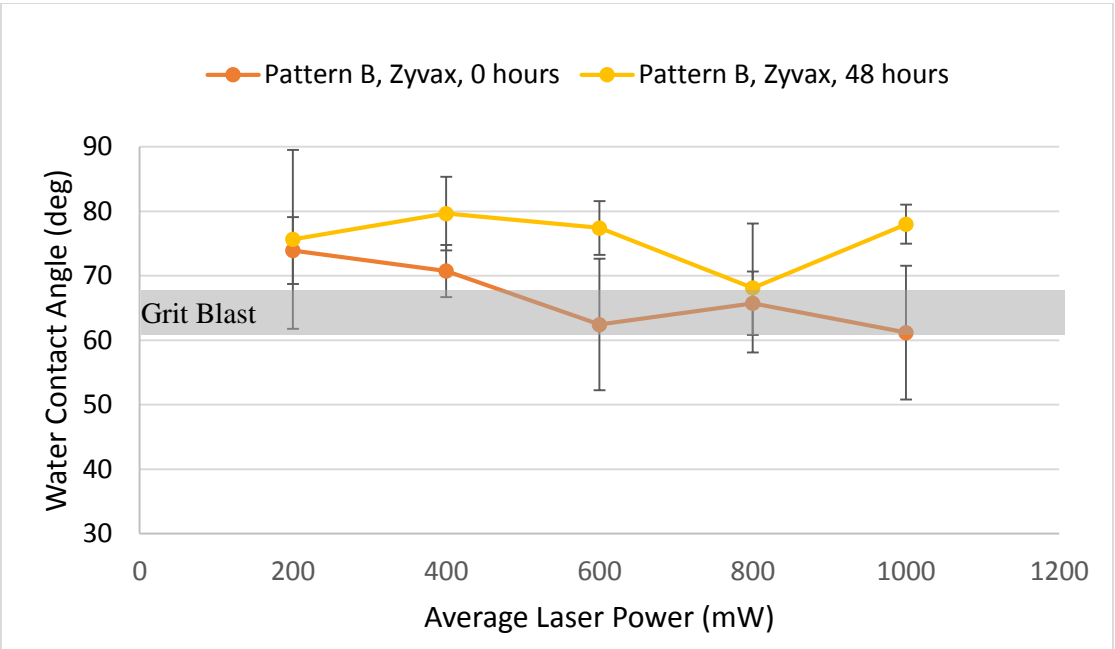


Figure 7: Water contact angle values for CFRP panels ablated with Pattern B immediately after ablation and just prior to adhesive bonding. The gray shaded area indicates the contact angle range measured for from the control sample that was prepared by grit blast.

### 3.3 Average Fracture Toughness and Failure Mode

#### 3.3.1 Average fracture toughness

Figure 8 shows the average fracture toughnesses measured from all experimental BB-DCB specimens normalized to the value for the grit blast control sample. Pattern A performed significantly better than Pattern B and met or exceeded the performance of the control specimen at 800 mW ablation power. The decrease in  $G_{AVG}$  for Pattern A at 1000 mW has been attributed to possible exposure or damage to carbon fibers at the surface due to excessive laser power. Exposure of the carbon fibers might have reduced the fracture toughness by providing a path for the crack front to move from the bondline into the top ply of the CFRP. Additionally, loose debris from damaged fibers might have reduced the bond interfacial properties. Pattern B did not achieve more than 80% of the control  $G_{AVG}$  value. This was attributed to incomplete areal coverage in Pattern B which left residual contamination on the surface. To achieve the toughness behavior observed in the control sample, the laser ablation process must achieve complete areal coverage with minimal exposure or damage of carbon fibers. Ideally, the goal is to selectively and completely remove surface contaminants while chemically activating only the top layer of resin. The high fidelity control associated with the laser ablation process should be fully capable of achieving this goal.

Samples fabricated with FEP mold release were only tested at 200 and 400 mW and Pattern A to minimize the number of experiments. At 200 mW, the  $G_{AVG}$  was approximately equal for the three surface conditions tested. Given the limited data set, it is not clear if the low areal coverage or the shallow ablation depth created at 200 mW is responsible for the poor bond performance. At 400 mW, the FEP molded panels showed a significant increase in  $G_{AVG}$  over the Zyx molded samples. This was attributed to less contamination on the surface from the molding process, which requires less ablation depth and areal coverage to remove. This observation is indicative of the sensitivity of bond performance to surface preparation and the need for a robust treatment process.

#### 3.3.2 Failure mode

Failure modes were determined visually using practices described in ASTM D5573. Trends in failure mode appear to correlate best with the calculated areal coverage data (Table 2). Nearly 100% cohesion failure was observed for both the control and experimental specimens with the highest areal coverage (Pattern A @ 1000 and 800 mW, Pattern B @ 1000 mW). For the 400 mW FEP specimens, either 100% cohesion failure or thin layer cohesion failure was observed, which might have caused the large uncertainty in the  $G_{AVG}$  value. Mixed-mode failures were observed for specimens that received moderate areal coverage (Pattern A @ 800 and 600 mW, Pattern B @ 800 mW). In specimens with the lowest areal coverage, predominantly adhesive failure was observed (Pattern A @ 200 mW, Pattern B @ 600, 400, and 200 mW). In specimens with the lowest areal coverage and ablation depth, predominantly adhesive failure was observed (Pattern A @ 200 mW, Pattern B @ 600, 400, and 200 mW, and Pattern A FEP @ 200 mW).

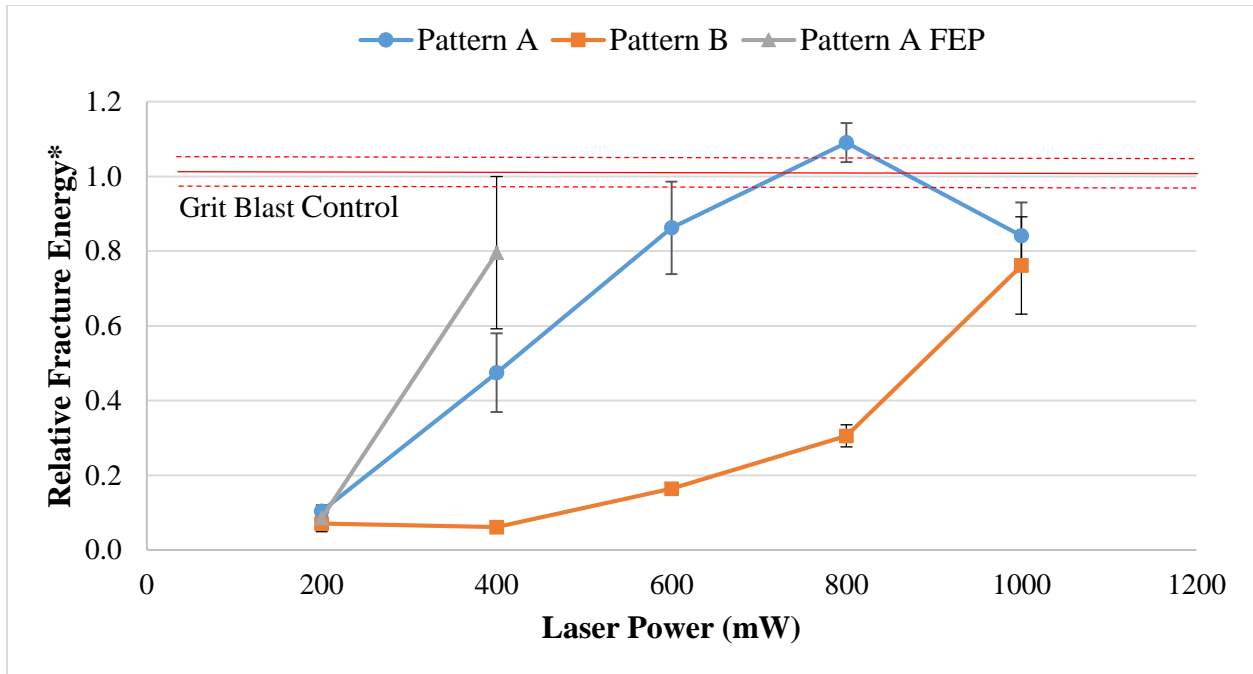


Figure 8. Average fracture energies measured from BB-DCB tests. \*Experimental fracture toughness values normalized to the control sample value.

### 3.4 Correlation of Results

The Pearson’s correlation coefficients (C) shown in Table 3 were calculated for laser power, average fracture toughness, water contact angle just prior to adhesive bonding (CA @ 48 h), and ablation trench depth and width. Correlation values were arbitrarily classified as either weak or strong according to the legend in Table 3 to aid discussion. The contact angle correlated weakly and inversely with all other variables. The low correlation values were due to the nearly constant contact angle measured for all panels just prior to adhesive bonding (Figures 6 and 7). The inverse correlation indicates that wetting improved (contact angle decreased), if only slightly, as the ablation power increased. Power and average fracture toughness correlated strongly although the decrease in fracture toughness for Pattern A at 1000 mW did not correlate. The depth and width of the ablation trench correlated strongly with both power and  $G_{AVG}$ . The strong correlation with power indicated the ability of the laser to control trench morphology. The strong correlation with  $G_{AVG}$  indicated the ability to control bond properties by tuning trench morphology. This enable adjustment of depth and width by tuning laser power in order to achieve optimum processing parameters.

Table 3: Correlations determined from Pattern A and Pattern B data, combined.

	$G_{AVG}$	CA @ 48 h	Depth	Width
Power	0.72	-0.28	0.95	0.94
$G_{AVG}$	1	-0.45	0.95	0.92
CA @ 48 h	na	1	-0.38	-0.34
Depth	na	na	1	0.99
Legend	weak: $0 < C \leq 0.6$ , strong: $0.61 \leq C \leq 1$			

## 4. CONCLUSIONS

Surface preparation of composites is a critical step to achieving high performance, durable adhesive bonds. Laser ablation is a high precision, reproducible, and automated method of preparing a CFRP surface for adhesive bonding with little or no waste stream. Based on electron microscopy data, average laser power can be tuned to accurately control the depth and width of ablation. The results indicate that ablation depth can be set at a predetermined value depending on surface contamination and resin thickness above the reinforcing fibers. This method can be customized for specific CFRP parts with different resin surface thickness to prevent or minimize the exposure of reinforcing fibers to the bondline. Water contact angle was significantly reduced after laser ablation, but the lowest observed values were typically not stable beyond 48 h. Bond performance in terms of fracture toughness and failure mode depended strongly on areal coverage by laser ablation. At approximately 100% areal coverage, bond performance compared well with state-of-the-art grit blast surface preparation. These results strongly suggest that laser ablation is a viable technology for large scale surface preparation where repeatable micron-scale depth control is critical to product yield. Similar laser systems with higher power and faster scanning optics are available for industrial scale manufacturing. Transition of this technique from laboratory coupon scale to manufacturing scale is the focus of ongoing research.

## 5. ACKNOWLEDGEMENTS

The Authors are grateful for the excellent support provided by Sean Britton, Hoa Luong, and Louis Simmons, all of NASA Langley Research Center, in the fabrication and characterization of the composite laminates and mechanical test specimens used in this work. The authors also thank Sean Ward of the Boeing Company for preparing the control specimens used in this work.

## 6. REFERENCES

1. Bossi, R. and Piehl, M. "Bonding Primary Aircraft Structures: The Issues." *Manuf. Eng.* 59(2011): 101-109.
2. Higgins, A. "Adhesive Bonding of Aircraft Structures." *Int. J. Adhes. Adhes.*, 20 (2000) 367-376.
3. Benard, Q., Fois, M., Grisel, M., Laurens, P. and Joubert, F. "Influence of the Polymer Surface Layer on the Adhesion of Polymer Matrix Composites." *Journal of Thermoplastic Composite Materials*, 22, 1 (2009) 51-61.
4. Kanerva, M. and Saarel, O. "The Peel Ply Surface Treatment for Adhesive Bonding of Composites: A Review." *Int. J. Adhes. Adhes.*, 43 (2013) 60-69.
5. Encinas, N. et al. "Surface Modification of Aircraft Used Composites for Adhesive Bonding." *Int. J. Adhes. Adhes.* 50 (2014): 157-163.
6. Fischer, F., Kreling, S., and Dilger, K. "Surface Structuring of CFRP by Using Modern Excimer Laser Sources." *Physics Procedia* 39 (2012) 154-160.
7. Wingfield, J. R. J., "Treatment of Composite Surfaces for Adhesive Bonding," *Int. J. Adhes. Adhes.* 13, 3 (1993) 151-156.
8. Fisher, F., Kreling, S., and Delmdahl, R. "Using Excimer Lasers to Clean CFRP Prior to Adhesive Bonding." *Reinforced Plastics* 57, 5 (2013) 43-46.

9. Benard Q. et al. "Surface Treatment of Carbon/Epoxy and Glass/Epoxy Composites with and Excimer Laser Beam." *International Journal of Adhesion and Adhesives*, 26, 7 (2006), 543-549.
10. Belcher, M.A. et al. "Laser Surface Preparation and Bonding of Aerospace Structural Composites" *55th International SAMPE Symposium and Exhibition* (2010) Seattle, WA.
11. Belcher, M.A., Wohl C.J. and Connell, J.W. "Surface preparation and bonding of composite aircraft" *32nd Annual Meeting of the Adhesion Society* (2009) Savannah, GA.
12. Parker, B. M., and Waghorne, R. M. "Surface Pretreatment of Carbon Fibre-reinforced Composites for Adhesive Bonding." *Composites*, 13, 3 (1982) 280-288.
13. Benard, Q., Fois, M., and Grisel, M. "Peel Ply Surface Treatment for Composite Assemblies: Chemistry and Morphology Effects." *Composites Part A: Applied Science and Manufacturing* 36 (2005) 1562-1568
14. Palmieri, Frank et al. "Laser Ablation Surface Preparation of Carbon Fiber Reinforced Epoxy Composites for Adhesive Bonding" *SAMPE 57 Technical Conference Proceeding*, Long Beach, CA May 6-9, 2013. Society for the Advancement of Material and Process Engineering, online proceedings <http://www.memberjournal.com/>.
15. ASTM D 5528-01, Standard Test Method for Mode I Interlaminar Fracture Toughness of Unidirectional Fiber-Reinforced Polymer Matrix Composites
16. Van Voast, Peter J. et al. "Rapid Test Methods for Adhesives and Adhesion," *SAMPE 57 Technical Conference Proceedings*, Long Beach, CA, May 6-9, 2013. Society for the Advancement of Material and Process Engineering, online proceedings <http://www.memberjournal.com/>.
17. ASTM D5573-99 and ASTM D5573-ADJ, Standard Practice for Classifying Failure Modes in Fiber-Reinforced-Plastic (FRP) Joints.